New Fluorescent Adenosine A_1-Receptor Agonists That Allow Quantification of Ligand−Receptor Interactions in Microdomains of Single Living Cells

Richard J. Middleton,[†,‡] Stephen J. Briddon,[‡,§] Yolande Cordeaux,[§] Andrew S. Yates,[†] Clare L. Dale,[†] Michael W. George,[∥] Jillian. G. Baker,[§] Stephen J. Hill,*[,§] and Barrie Kellam*[,†]

School of Pharmacy, Centre for Biomolecular Sciences, and School of Chemistry, University of Nottingham, University Park, Nottingham, United Kingdom, NG7 2RD, and Institute of Cell Signalling, Medical School, University of Nottingham, Nottingham, United Kingdom, NG7 2UH

Received November 2, 2006

Fluorescence spectroscopy is becoming a valuable addition to the array of techniques available for scrutinizing ligand−receptor interactions in biological systems. In particular, scanning confocal microscopy and fluorescence correlation spectroscopy (FCS) allow the noninvasive imaging and quantification of these interactions in single living cells. To address the emerging need for fluorescently labeled ligands to support these technologies, we have developed a series of red-emitting agonists for the human adenosine A_1-receptor that, collectively, are N^6-aminoalkyl derivatives of adenosine or adenosine 5′-*N*-ethyl carboxamide. The agonists, which incorporate the commercially available fluorophore BODIPY [630/650], retain potent and efficacious agonist activity, as demonstrated by their ability to inhibit cAMP accumulation in chinese hamster ovary cells expressing the human adenosine A_1-receptor. Visualization and confirmation of ligand−receptor interactions at the cell membrane were accomplished using confocal microscopy, and their suitability for use in FCS was demonstrated by quantification of agonist binding in small areas of cell membrane.

Introduction

G-protein coupled receptors (GPCRs[a]) represent the largest family of cell-surface receptors mediating cellular communication and are a major target for drugs in current clinical use.[1] The endogenous ligands for GPCRs are a diverse range of hormones, transmitters, autocrine factors, and even photons. In each case, however, the receptor transduces the binding of ligand to an intracellular signal via activation of a heterotrimeric guanosine triphosphate-binding protein (G-protein). As a consequence of this, a range of downstream intracellular signals are activated, resulting in both short-term effects (e.g., changes in cellular calcium levels) and long-term effects (e.g., gene transcription). The nucleoside adenosine is one such ligand, for which there are four characterized GPCRs (A_1-, A_{2A}-, A_{2B}-, and A_3-receptors).[2] The adenosine A_1-receptor (A_1-AR) is responsible for mediating the physiological effects of adenosine in diverse tissues such as the brain, heart, kidney, and adipocytes[2] and signals via G-proteins of the $G_{i/o}$ family to inhibit adenylyl cyclase and thus reduce cellular levels of cyclic adenosine monophosphate (cAMP). Our current understanding of A_1-AR pharmacology has arisen predominantly from the use of conventional techniques for investigating ligand−receptor interactions, such as radioligand binding and standard assays of receptor function, which involve metabolic labeling. These experiments require large numbers of cells and give a population average for the pharmacological parameters they determine. However, it is now evident that A_1-ARs are not uniformly distributed at the cell surface but, instead, are organized within membrane compartments and microdomains,[3] providing a mechanism by which intracellular signaling can be orchestrated in different areas of an individual cell. Studying the pharmacology of such receptor subpopulations is beyond the scope of such traditional radioligand binding assays.

The introduction of fluorescence-based techniques such as confocal microscopy and fluorescence correlation spectroscopy (FCS) has progressed the study of GPCR pharmacology to the single cell level[4] and to the point where domain-specific receptor pharmacology can realistically be investigated. Specifically, FCS records fluctuations in photon emission as a fluorescent molecule diffuses through a diffraction limited excitation volume (∼0.5 fL) created by a highly focused laser beam. Statistical analysis of such fluctuations allows the concentration and diffusional characteristics of these fluorescent molecules to be determined.[5] Because FCS is noninvasive, sensitive, and quantitative, it is ideal for use in living cells and has been employed successfully to measure the diffusion of both genetically and chemically labeled proteins.[6] The ability of FCS to distinguish between fast-moving small molecule ligands and their slower moving receptor-bound forms has been exploited to perform single-cell pharmacology.[5b,7,8] To apply this technique to the study of GPCRs, there is a clear prerequisite to fluorescently label the receptors and the molecules that interact with them. In particular, for the quantification of ligand−receptor interactions, there is a specific need for fluorescent ligands with appropriate photochemical and pharmacological properties.[9] To this end, we have recently demonstrated this approach in the synthesis and

* To whom correspondence should be addressed. Tel.: +44-115-951-3026 (B.K.); +44-115-8230082 (S.J.H.). Fax: +44-115-9513412 (B.K.); +44-115-8230081 (S.J.H.). E-mail: barrie.kellam@nottingham.ac.uk (B.K.); stephen.hill@nottingham.ac.uk (S.J.H.).

† School of Pharmacy.

‡ These authors contributed equally to this work.

§ Institute of Cell Signalling, Medical School.

∥ School of Chemistry.

[a] Abbreviations: cAMP, cyclic adenosine monophosphate; AR, adenosine receptor; BAIB, bis(acetoxy)iodobenzene; BODIPY 630/650 or BY630, 6-(((4,4-difluoro-5-(2-thienyl)-4-bora-3a,4a-diaza-*s*-indacene-3-yl)styryloxy)acetyl)amino-hexanoic acid; BODIPY 630/650-X, SE, 6-(((4,4-difluoro-5-(2-thienyl)-4-bora-3a,4a-diaza-*s*-indacene-3-yl)styryloxy)acetyl)amino-hexanoic acid succinimidyl ester; CHO, chinese hamster ovary cell; CPA, N^6-cyclopentyladenosine; DIEA, di-isopropylethylamine; DMF, *N*,*N*-dimethylformamide; DMP, 2,2-dimethoxypropane; DPCPX, 1,3-di-*n*-propyl-8-cyclopentylxanthine; FCS, fluorescence correlation spectroscopy; GPCRs, G-protein coupled receptors; NECA, adenosine 5′-*N*-ethyl carboxamide; τ_D, diffusion time; TEMPO, 2,2,6,6,tetramethyl-1-piperidinyloxy free radical; THF, tetrahydrofuran; XAC, xanthine amine congener; Z, benzyloxycarbonyl.

10.1021/jm061279i CCC: $37.00
Published on Web 01/24/2007

Scheme 1[a]

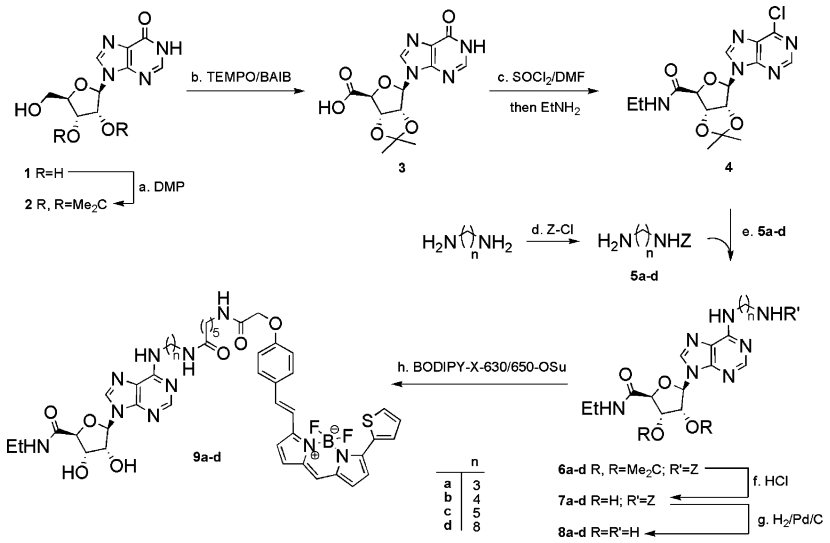

[a] Reagents and conditions: (a) DMP, tosic acid, acetone, rt, 18 h, 60%; (b) BAIB, TEMPO, MeCN/water (1:1), rt, 2 h, 83%; (c) (i) $SOCl_2$, DMF, $CHCl_3$, reflux, 5 h (ii) $EtNH_2$, THF, 5 °C to rt, 30 min, 60−90%; (d) Z-Cl, $CHCl_3$, rt, 18 h, 35−65%; (e) **5a**−**d**, DIEA, EtOH reflux, 18 h, 70−85%; (f) 1 M $HCl_{(aq)}$/1,4-dioxane (1:1), 70 °C, 4 h, 60−70%; (g) H_2/Pd/C, MeOH/water/AcOH (9.0:0.9:0.1), rt, 3 h, quantitative; (h) BODIPY-X-630/650-OSu, DMF, rt, 4 h, 75−85%.

characterization of a novel fluorescent antagonist, XAC-BY630 ((*E*)-*N*-(2-(2-(4-(2,6-dioxo-1,3-dipropyl-2,3,6,7-tetrahydro-1*H*-purin-8-yl)phenoxy)acetamido)ethyl)-6-(2-(4-(2-(4,4-difluoro-4,4a-dihydro-5-(thiophen-2-yl)-4-bora-3a,4a-diaza-*s*-indacene-3-yl)vinyl)phenoxy)acetamido)hexanamide), for the A_1-AR.[10] This compound retained the antagonist properties of xanthine amine congener (XAC), while also allowing visualization of the A_1-AR and detection of antagonist−receptor complexes in small areas of cell membrane using FCS. It was our intention, therefore, to complement this approach by developing fluorescent ligands for the A_1-AR receptor that possess both appropriate fluorescent properties for FCS but also have agonist activity at the receptor.

A large proportion of fluorescent agonists for GPCRs thus far described are peptide-based.[11] For these ligands, the conjugated fluorophore constitutes a relatively small component of the overall molecule and can be positioned such that it is well separated from the pharmacophore. However, in the case of GPCRs activated by biogenic amines, the ligand binding sites are buried within the transmembrane regions of the receptor and interact with much smaller molecules. Consequently, appropriate positioning of the fluorophore within the final conjugate is critical to retain both receptor binding affinity and efficacy. Given the high fidelity of ligand−receptor interactions, it is imperative that new fluorescent derivatives are characterized as novel pharmacological entities in their own right rather than assuming that they retain the properties of the parent ligand.[12]

Our goal to generate fluorescent agonists for the human A_1-AR initiated a review of the structure−activity relationships of the native ligand adenosine and its derivatives. For this receptor, modifications to the N^6-position of adenosine and the structurally similar agonist adenosine 5′-*N*-ethyl carboxamide (NECA) are well tolerated, yielding ligands that retain biological activity.[13] This allows insertion of N^6-aminoalkyl spacers of various chain lengths to yield the corresponding functionalized congeners that are amenable to fluorescent labeling. Examples of fluorescently labeled derivatives of agonists targeted at the A_1-AR have been described using this approach, but their agonist activity, to the best of our knowledge, is yet to be reported. Additionally, the UV-excited fluorophores employed in these studies are unsuitable for use with FCS.[14] In comparison, the use of a fluorophore that possesses a longer excitation wavelength will help to minimize autofluoresence and maximize flexibility for use in multicolor applications with fluorescent protein labels.

In this paper, we describe the synthesis of new red-emitting fluorescent agonists for the A_1-AR. We show that they are potent and efficacious as agonists, and we demonstrate their use in monitoring and quantifying agonist−receptor interactions in single living cells. Specifically, the congeners belong to a series of N^6-aminoalkyl NECAs and an N^6-aminoalkyladenosine.

Results and Discussion

Synthesis. Following the general theme of Olsson,[13a] inosine **1** was protected as the corresponding 2′,3′-isopropylidene ketal with 2,3-dimethoxypropane and tosic acid (Scheme 1). Crystallization of ketal **2** from water provided a convenient purification and proved to be a key determinant in its subsequent efficient oxidation to **3**. While most nucleoside 5′-hydroxymethyl oxidations of this type have relied on metal-based reagents (Mn, Cr), Epp and Widlanski have reported a facile preparation utilizing the in situ generation of the *N*-oxoammonium salt derived from TEMPO.[15]

Under these conditions and with high concentrations of water,[16] aliphatic alcohols are converted to their respective carboxylic acids, and the oxidation of 2′,3′-isopropylidene-nucleosides (adenosine, uridine, cytidine, and guanosine) was reported in high yield.[15] Furthermore, the reaction generates only acetic acid and iodobenzene as byproducts, which are easily removed from the precipitated product by trituration to yield the acids in analytical purity.

Initial attempts of the synthesis of acid **3** from noncrystalline **2** resulted in a successful transformation but required long reaction times and afforded lower purities than anticipated.[15] In contrast to the previously investigated nucleosides, addition of base or lowering of the reaction temperature did not elicit a substantial improvement.[15] However, substituting crystalline **2** into the reaction afforded acid **3** in 2 h in high yield and analytical purity after trituration of the crude product with acetone and diethyl ether. To the best of our knowledge, this constitutes the first extension of this methodology to inosine nucleosides and represents a major improvement in the chemical

Scheme 2[a]

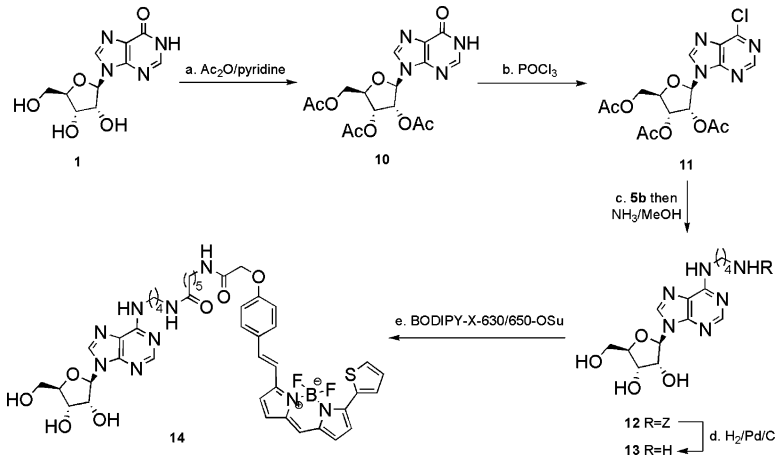

[a] Reagents and conditions: (a) Ac_2O, pyridine, 40 °C, 1 h, 97%; (b) $POCl_3$, *N*,*N*-dimethylaniline, reflux, 5 min, 85%; (c) (i) **5b**, DIEA, EtOH reflux, 18 h; (ii) NH_3/MeOH, 0 °C, 2 h, 66%; (d) H_2/Pd/C, MeOH/water/AcOH (9.0:0.9:0.1), rt, 3 h, quantitative; (g) BODIPY-X-630/650-OSu, *N*,*N*-DMF, rt, 4 h, 75%.

repertoire available for the synthesis of adenosine derivatives. Indeed, high-yielding, multigram preparations of **3** are now routinely carried out in our laboratories without the need for chromatographic or laborious purifications.

For the introduction of C5′- and N^6-substituents, there exist a number of reagents that may be used sequentially to effect the required chlorination and carboxyl activation/amidation reactions. We chose, however, to attempt simultaneous chlorination at these positions and exploit the susceptibility of the resultant acyl and aryl halides toward regioselective amine displacement under temperature control. This approach, as described by Olsson et al., using DMF/$SOCl_2$,[13a] has been both reproduced[13b,c,e,14a,b] and described as not favorable under the reported reaction conditions.[13d] Following minor experimental modifications, we were able to isolate the uronamide derivative **4** in good yield following low temperature in situ ethylamine-mediated aminolysis of the C4′-acid chloride. The reaction remains highly sensitive to the quality of reagents employed, however, and demands carefully determined reaction conditions in return for a high-yielding transformation.

Displacement of the 6-chloro group with a variety of monoprotected alkyl diamines **5a**−**d** furnished the N^6-aminoalkyl NECAs **6a**−**d** thus introducing the linker unit and chemical functionality for conjugation with the fluorophore. The mono-Z-protected diamines **5a**−**d** are available via the reaction of a large excess of the corresponding diamines with benzyl chloroformate under pseudo-dilution conditions. An aqueous acid extraction effects good separation of the desired linkers **5a**−**d** from the excess of diamine and bis-Z-protected byproduct.

It was our objective at this stage to remove all protecting groups prior to conjugation of the ligands with the fluorophore; this strategy has two distinct advantages. Due to the high cost of the commercially available fluorophores and, hence, the micromole conjugation reactions commonly employed, it is desirable to conjugate as the last synthetic step of a sequence. This reduces the synthetic loss of valuable intermediates and eliminates exposure of the often-fragile fluorophores to the rigorous conditions of chemical deprotections. Second, fully deprotected congeners present the opportunity for the facile, single-step synthesis of variously labeled ligands bearing a range of fluorophores or other "tagging" moieties. We envisaged initial ketal deprotection more appropriate, leaving the protected amine of **7a**−**d** as a suitable handle to assist purification of the resultant diol.

Removal of the ketal protecting group was effected with 1 N HCl in aqueous dioxane at 70 °C in moderate to good yields, with diols **7a**−**d** readily purified by preparative layer chromatography. Hydrogenolysis of the *N*-benzyloxycarbonyl group effected a near-quantitative recovery of amines **8a**−**d** in sufficient purity to be labeled directly. Surprisingly, initial attempts at the Z-deprotection yielded *N*-methyl derivatives of the desired primary amines **8a**−**d**, which were observed by mass spectrometry. Similar alkylations have been described in the literature and arise from the conversion of methanol to formaldehyde in the presence of the palladium catalyst and subsequent reductive amination under the prevailing reducing conditions.[17] This alkylation was easily suppressed by inclusion of aqueous acid in the solvent mixture.

Conjugation of an excess of the congeners **8a**−**d** with the commercially available amine-reactive fluorophore 6-(((4,4-difluoro-5-(2-thienyl)-4-bora-3a,4a-diaza-*s*-indacene-3-yl)styryloxy)acetyl)amino-hexanoic acid, succinimidyl ester (BODIPY 630/650-X, SE; Molecular Probes) proceeded smoothly, and the fluorescently labeled ligands **9a**−**d** were isolated by preparative layer chromatography and their purity was confirmed by RP-HPLC with photodiode-array detection from 190 to 800 nm.

The synthesis of the N^6-aminobutyladenosine derivative **14** followed a similar synthetic strategy (Scheme 2). The potential for this ligand to interact with other nonreceptor adenosine binding sites (e.g., adenosine transporters) is likely to be higher than the corresponding uronamide derivatives; **14** was synthesized, however, to test whether there was a benefit in terms of increased potency or efficacy (cf. the selectivity of N^6-cyclopentyladenosine (CPA) for the A_1-AR).[18] Peracetylation of inosine under standard conditions was followed by chlorination at C6 using $POCl_3$. Displacement of the resultant 6-chloro group with the mono-Z-protected diamine **5b** also effected partial deacetylation via simple $O \rightarrow N$ acyl transfer, with the nucleoside mono- and diacetates being clearly distinguished by thin layer chromatography (TLC). Global acetate deprotection was therefore effected using an alcoholic solution of ammonia to afford N^6-(benzyloxycarbonylaminobutyl)adenosine **12** in good yield. Hydrogenolysis and fluorophore conjugation followed without incident, providing the fluorescent derivative **14** after preparative layer chromatography.

We have previously labeled a small molecule GPCR antagonist with the commercially available fluorophore BODIPY [630/650] and demonstrated its suitability for use in FCS.[10] This

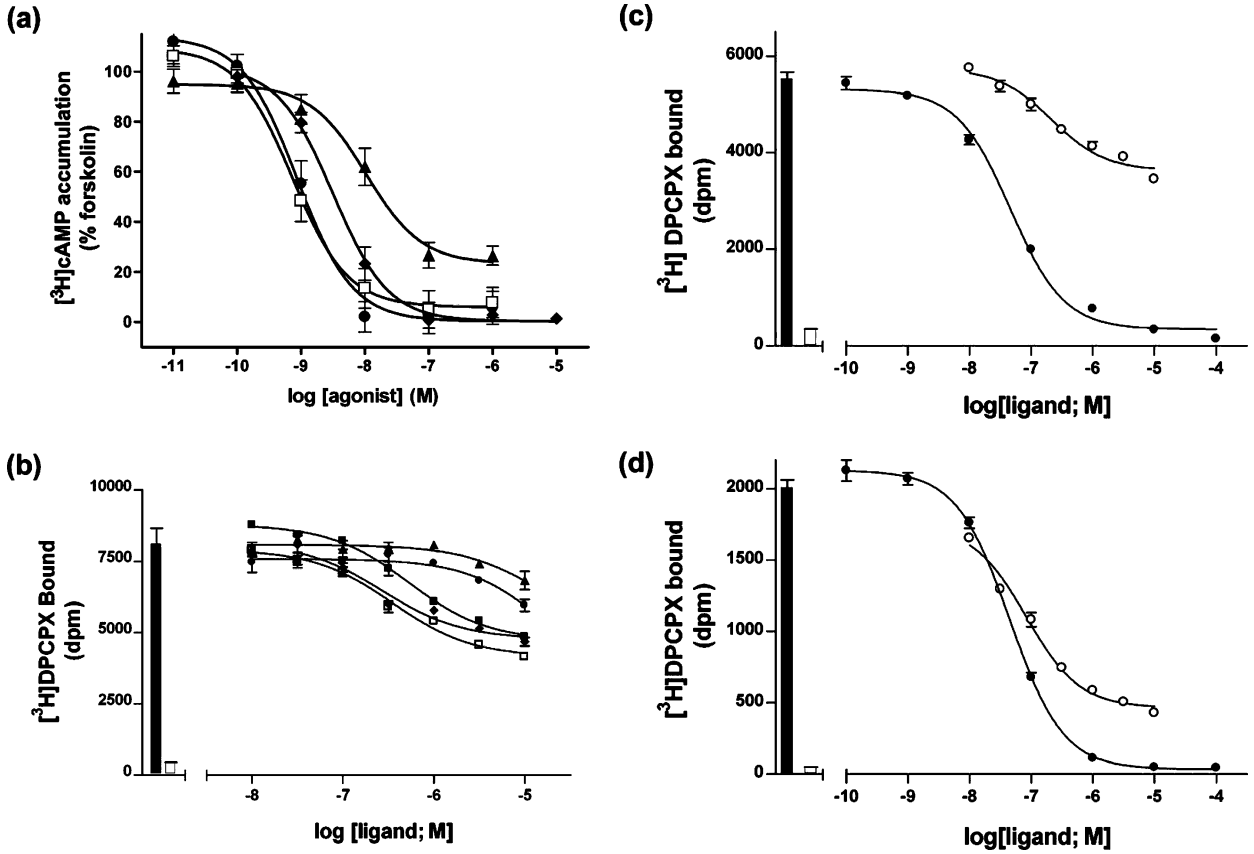

Figure 1. Radioligand binding and functional analysis of fluorescent adenosine derivatives in CHO-A1H cells. (a) Inhibition of [^{3}H]-cAMP accumulation by **9a**−**d**. Stimulation of [^{3}H]-cAMP accumulation (from [^{3}H]-adenine) is expressed as a percentage of that obtained with 3 μM forskolin. Each point represents mean ± s.e. mean obtained from three independent experiments, performed in triplicate with **9a** (□), **9b** (♦), **9c** (●), and **9d** (▲). (b) Competition radioligand binding data in CHO-A1H cells using [^{3}H]-DPCPX as radioligand. Total binding is shown in the filled bar and nonspecific binding (in the presence of 10 μM XAC) is shown in the open bar. Data are shown as mean ± s.e. mean triplicates within an experiment representative of eight (**9a**−**d**) or six (**14**) performed. The key to symbols is as described for (a) and **14** (■). (c) Competition radioligand binding data in intact CHO-A1H cells for XAC (●) and **9b** (○) using [^{3}H]-DPCPX as radioligand. Total and nonspecific binding are illustrated as in (b). Data are shown as mean ± s.e. mean triplicates within an experiment representative of four performed. (d) Experiments performed as in (c) but with cells permeabilized with 0.01% Triton-X100.

Table 1. Concentration-Response and Ligand-Binding Parameters for Fluorescent Agonists Acting at the Human A_1-Adenosine Receptor[a]

	[^{3}H]-cAMP accumulation			[^{3}H]-DPCPX binding			
ligand	−log EC_{50} (A)	% maximal inhibition of forskolin response	*n*	−log K_D (B)	% maximal inhibition of specific binding	*n*	A−B
NECA	9.44[b]	98[b]		6.24 ± 0.04	83.3 ± 1.2	8	3.20
9a	9.16 ± 0.08	92 ± 5%	4	6.61 ± 0.10	50.9 ± 2.4	8	2.55
9b	8.47 ± 0.08	99 ± 1%	3	6.80 ± 0.11	49.3 ± 1.7	8	1.67
9c	9.15 ± 0.12	96 ± 3%	3	[c]	[c]	8	
9d	7.92 ± 0.15	77 ± 4%	4	[c]	[c]	8	
14	8.29 ± 0.05	96 ± 2%	3	6.65 ± 0.09	48.1 ± 3.9	6	1.64

[a] Concentration-response parameters were determined from inhibition of forskolin-stimulated (3 μM) [^{3}H]-cAMP accumulation. Ligand-binding parameters were determined from inhibition of the binding of 1 nM [^{3}H]-DPCPX. Values are mean ± s.e. mean from *n* separate experiments. [b] The values for NECA were taken from ref 20. [c] The inhibition curves for **9c** and **9d** were insufficiently defined at concentrations up to 10^{-5} M to determine ligand-binding parameters.

fluorescent moiety is bright, photostable, and has low triplet-state population.[19] In addition, cells do not exhibit high levels of autofluorescence or suffer from significant phototoxicity when exposed to its peak excitation wavelength. To ensure that conjugation of the fluorophore to the precursor molecules had not affected its photochemical properties, we measured the excitation/emission maxima of the five conjugates **9a**−**d** and **14**. None of these values differed significantly from that of the free fluorophore (637/658 nm; data not shown).

Pharmacology

Inhibition of [^{3}H]-cAMP Accumulation and [^{3}H]-DPCPX Binding in Chinese Hamster Ovary (CHO)-A1H Cells. To determine the potency and efficacy of the fluorescent agonists **9a**−**d** and **14** at the human A_1-AR, we evaluated their ability to inhibit forskolin-stimulated cAMP accumulation in CHO cells expressing this receptor (CHO-A1H cells), as described previously.[20] All five compounds produced a concentration-dependent inhibition of cAMP accumulation with an EC_{50} in the nanomolar range (Figure 1, Table 1).[21] The striking feature of these data was that all molecules displayed agonist activity. Apart from **9d**, all compounds produced over 90% inhibition of the forskolin response. This was similar to that previously obtained with NECA.[20] However, **9d** appeared to be a lower efficacy agonist in this system and interestingly was the least potent. To demonstrate that these responses were mediated via the A_1-

Table 2. $-\text{Log } EC_{50}$ Values for NECA or **9b** Stimulation of [^{3}H]-Cyclic AMP Accumulation (A_{2A}, A_{2B}) and Inhibition of Forskolin-Stimulated (3 μM) Cyclic AMP Accumulation (A_1, A_3) in CHO K1 Cells Expressing the Human A_1, A_{2A}, A_{2B}, or A_3 Adenosine Receptor[a]

	$-\text{Log } EC_{50}$ (n)	
adenosine receptor	NECA	**9b**
A_1	9.44[b]	8.47 ± 0.08 (3)
A_{2A}	7.76 ± 0.02 (3)	6.76 ± 0.06 (3)
A_{2B}	5.44 ± 0.22 (3)	5.69 ± 0.18 (3)
A_3	8.34 ± 0.12 (4)	8.57 ± 0.22 (5)

[a] Values represent mean ± s.e. mean from n separate experiments, each performed in triplicate. [b] The value for NECA was taken from ref 20.

AR, parallel experiments were performed with **9b** and **14** following preincubation of the cells with the selective A_1-AR antagonist 1,3-di-*n*-propyl-8-cyclopentylxanthine (DPCPX; pK_B = 7.85 ± 0.01 and 7.91 ± 0.06, n = 3, respectively).[21] The affinity values obtained from these functional assays for DPCPX are consistent with those previously demonstrated in this cell line.[20] It was evident from these data that **14** displayed similar agonist potency and efficacy when compared to the corresponding uronamide derivative **9b**. As a consequence, further studies on variations in linker length were undertaken solely on the uronamide series.

To gain some insight into the selectivity of this series of compounds for the different adenosine receptors, we evaluated the ability of **9b** to stimulate cAMP accumulation via adenosine-A_{2A} and -A_{2B} receptors expressed in CHO-K1 cells and to inhibit forskolin-stimulated cAMP via adenosine-A_3 receptors expressed in the same cell background (Table 2). These data show that **9b** has a very similar potency on Gi-coupled A_3- and A_1-receptors, but is much less potent as an agonist of the Gs-coupled A_{2A}- and A_{2B}-receptors.

Whole cell binding studies with [^{3}H]-DPCPX in CHO-A1H cells yielded a K_D value for [^{3}H]-DPCPX of 1.92 ± 0.23 nM (n = 6). NECA inhibited the specific binding (defined as that displaceable by 10 μM XAC) of [^{3}H]-DPCPX by 83.3 ± 1.5% to yield a $-\log K_D$ value of 6.24 ± 0.04 (n = 8; Table 1). Compounds **9a**, **9b**, and **14** inhibited [^{3}H]-DPCPX binding to reach a clear plateau at about 50% of the specific binding displaced by XAC (Figure 1b; Table 1). Estimation of the $-\log K_D$ values for this component of binding indicated that these three ligands showed similar affinities for the A_1-receptor. Unfortunately, there was not sufficient displacement of [^{3}H]-DPCPX binding at concentrations of **9c** and **9d** below 10 μM to allow confident estimation of ligand-binding parameters for these two compounds (Figure 1b). A potential explanation for the partial displacement of specific [^{3}H]-DPCPX binding by **9a**, **9b**, and **14** is that both [^{3}H]-DPCPX and XAC are able to cross the cell membrane and bind to intracellular A_1-receptors, whereas **9a**, **9b**, and **14** are relatively less membrane permeable. To test this hypothesis, we directly compared the degree of maximum displacement of specific [^{3}H]-DPCPX binding obtained in intact CHO-A1H cells with that achieved in CHO-A1H cells that had been permeabilized with 0.01% Triton-X100 (Figure 1c,d). These data confirmed that the maximum displacement of specific [^{3}H]-DPCPX binding (defined with XAC) obtained with **9b** increased from 49.3 ± 1.7 to 75.6 ± 2.5% (Figure 1c,d) with no significant change in the apparent $-\log K_d$ values (6.80 ± 0.11 and 7.13 ± 0.08; n = 8 and 4, respectively).

It was evident in the functional cAMP assays that the structure−activity relationship for the uronamide series demonstrated a dependence of potency on the odd/even nature of the linker (Table 1). This is likely to be related to agonist efficacy rather than affinity because the ligand binding affinities were quite similar for **9a**, **9b**, and **14**. To gain some insight into this, the difference between the $-\log EC_{50}$ and $-\log K_D$ values have been presented in Table 1 as an indicator of agonist efficacy (on a logarithmic scale). It is notable that **9b** and **14** share very similar efficacies and potencies on this basis.

Confocal Imaging of Ligand Binding. Having demonstrated the high potency of **9a**−**d** in functional assays, we were able to use these compounds to visualize ligand−receptor interactions using confocal microscopy (Figure 2a). These experiments were performed at 22 °C to minimize receptor internalization and thus maximize the signal seen on the cell membrane. Incubation of CHO-A1H cells with **9a**−**d** resulted in a clear labeling of the cell membrane, which was time- and concentration-dependent. When added at 100 nM, membrane binding was seen as little as 5 min after addition of the drug and did not increase substantially after this time (data not shown). The degree of membrane binding seen following addition of each compound (100 nM, 10 min) was dependent on the length of the linker, with **9b** and **9c** showing the highest and **9d** showing the lowest level of specific binding (Figure 2a). None of the compounds showed any substantial intracellular binding at the times and concentrations tested. In each case, a substantial proportion of this binding was prevented by preincubation with DPCPX (100 nM, 30 min, 37 °C) and, hence, was specific binding to the A_1-AR. The binding of **9a**−**d** (100 nM, 10 min) to the A_1-AR was investigated further using CHO cells expressing the A_1-AR fused on its C-terminus to the Topaz variant of green fluorescent protein.[10] Again, for each compound, significant membrane binding was seen, and this binding co-localized with the fluorescent membrane-localized receptor. Preincubation of cells with DPCPX (100 nM) caused a significant decrease in both overall membrane binding and, more specifically, a large decrease in the co-localization seen between ligand and receptor (illustrated for **9b** in Figure 2b).

Quantification of Ligand Binding Using FCS. To quantify the binding of these ligands to the A_1-AR in nonspecified membrane microdomains of single cells, we used FCS. This technique analyzes the fluctuation in fluorescence signal as a fluorescent species diffuses through a small, defined confocal detection volume. Autocorrelation analysis of these fluctuations provides information on both the diffusion characteristics of the molecule (related to mass) and also the average number of molecules in the detection volume during the measurement (i.e., concentration). For the purposes of detecting ligand−receptor interactions, the detection volume can be positioned on the upper membrane of the cell. Here fluctuations from both fast-moving free-ligand molecules and slower-moving receptor-bound molecules will be detected simultaneously and their concentrations calculated. Thus, both (actual) free and bound ligand concentrations can be quantified in a small (~0.1 μm^2) area of membrane.[5b] Compounds **9a**−**d** all proved suitable for FCS measurements in aqueous solution, showing monophasic autocorrelation curves, with diffusion times of 69 ± 3 μs, 71 ± 3 μs, 72 ± 4 μs, and 74 ± 4 μs, respectively (n = 4; data not shown). All had triplet state populations of less than 7%, equivalent to the free fluorophore. FCS measurements were also taken on the upper membrane of CHO-A1H cells which had been incubated with **9b** as previously described.[22] Following positioning in x and y planes, the excitation volume was positioned in the upper membrane using intensity scanning in the z plane, where the peak corresponding to the upper membrane was clearly visible (Figure 3a).

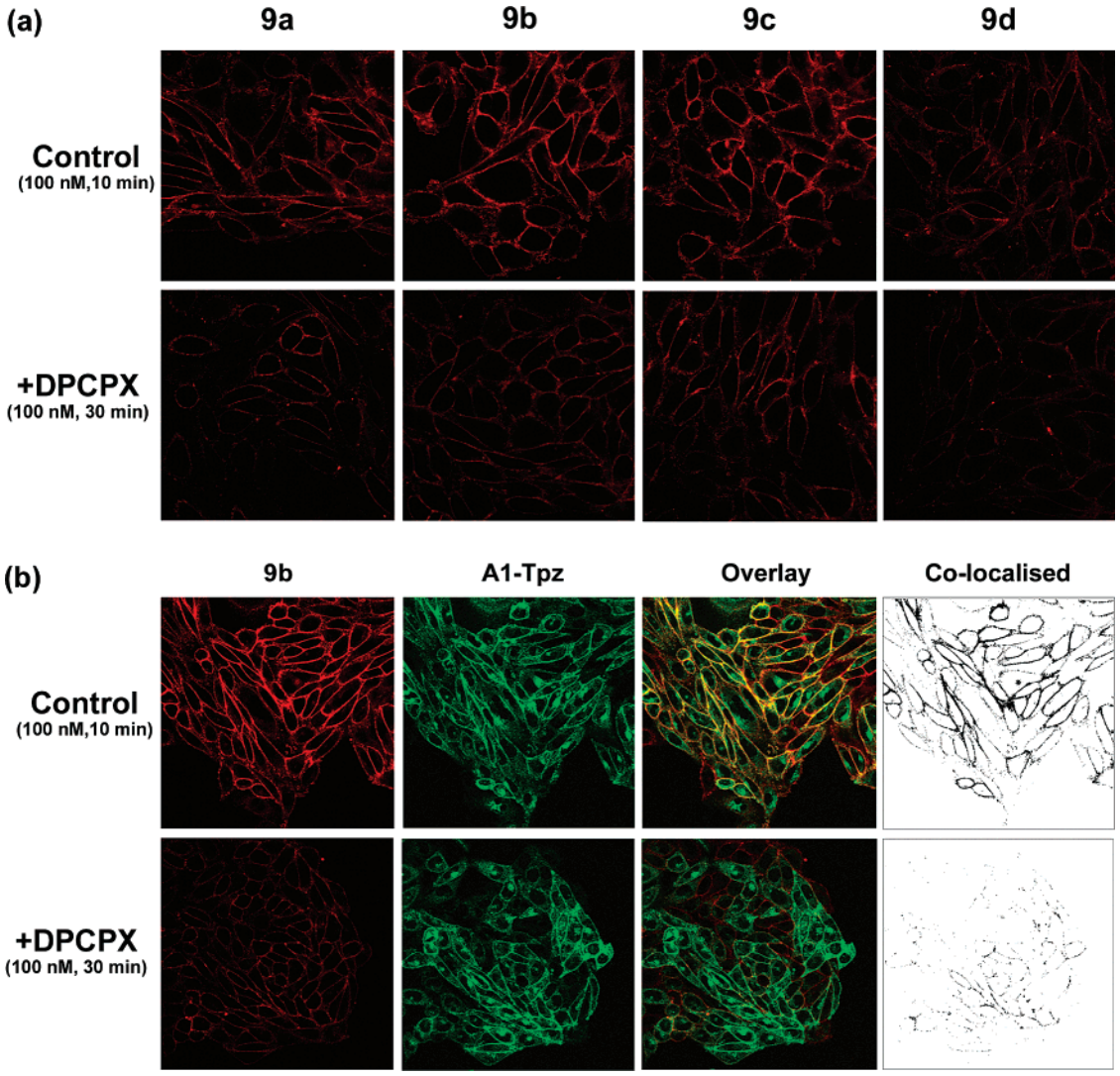

Figure 2. Visualizing fluorescent agonist binding using live cell confocal microscopy. (a) Top panel: CHO-A1H cells were incubated with fluorescent ligand (100 nM, 10 min, 22 °C) and single equatorial confocal images taken as previously described.[10] Lower panel: Similar experiments were performed on cells preincubated with the nonfluorescent A_1-AR antagonist, DPCPX (100 nM, 30 min, 37 °C). Images shown are from a single experiment within which identical settings for laser power, offset, and gain were applied. These data are representative of five (upper) or four (lower) experiments performed. (b) Experiments as above were performed using CHO cells expressing an A_1-AR fused on its C-terminus to Topaz fluorescent protein, with images obtained by simultaneous excitation with 488 and 633 nm, as previously described.[10] Ligand (red), receptor (green), and overlay images are shown, with yellow indicating co-localized pixels. For ease of viewing, these pixels are indicated in black in the final panel. The experiment shown is representative of three performed.

When positioned 2 μm above the cell membrane, the autocorrelation curve was monophasic, with a diffusion time of 67 ± 1 μs (n = 16), equivalent to that seen for this compound in aqueous solution (Figure 3b). However, positioning of the volume on the upper cell membrane results in an autocorrelation curve containing two further slow-diffusing components, which over a range of concentrations of **9b** (2−20 nM) were 9.5 ± 0.3 ms (τ_{D2}) and 267 ± 27 ms (τ_{D3}; n = 47; Figure 3c). Similar diffusion components were identified when using a fluorescent antagonist ligand for the A_1-AR[10] and also for **9a**, **c**, and **d** (data not shown). To determine whether these diffusion components represented receptor−ligand complexes, measurements were made on cells exposed to **9b** (5 nM) in the presence or absence of DPCPX (100 nM, 30 min, 37 °C) and the amount of τ_{D2} and τ_{D3} quantified. As shown in Figure 4a, the level of total binding on CHO-A1H cell membranes was significantly greater than that seen in native CHO-K1 cells. This binding was to the A_1-AR because it was significantly inhibited by preincubation with a selective concentration of DPCPX (100 nM). Similar experiments in CHO-A2B cells (Figure 4a) demonstrated that, at this concentration of **9b**, there was no significant binding to the A_{2B}-AR in CHO cell membranes. Therefore, using the low concentrations of ligand required for FCS, it should be achievable to selectively measure the binding to the A_1-AR in cells endogenously expressing the A_{2B}-AR. Binding of **9b** to the CHO-A1 cells consisted of approximately 40% τ_{D2} and 60% τ_{D3} (Figure 4b). DPCPX significantly reduced the amount of both of these binding components, suggesting that both τ_{D2} and τ_{D3} represent the diffusion of ligand−receptor complexes. This is consistent with previous reports of agonist binding using peptide ligands.[8,23] Diffusion times for τ_{D2} and τ_{D3} were slightly faster in the cells, which had been pretreated with DPCPX (τ_{D2} = 8.1 ± 0.2 and 7.1 ± 0.2 ms and τ_{D3} = 243 ± 10 and 151 ± 7 ms, in control and DPCPX-treated cells, $P < 0.05$ and $P < 0.01$, respectively). Though the exact nature of these species is yet to be determined, they may represent, for instance, diffusion of the receptor within different membrane microdomains or the diffusion of the receptor superimposed on that of a microdomain.

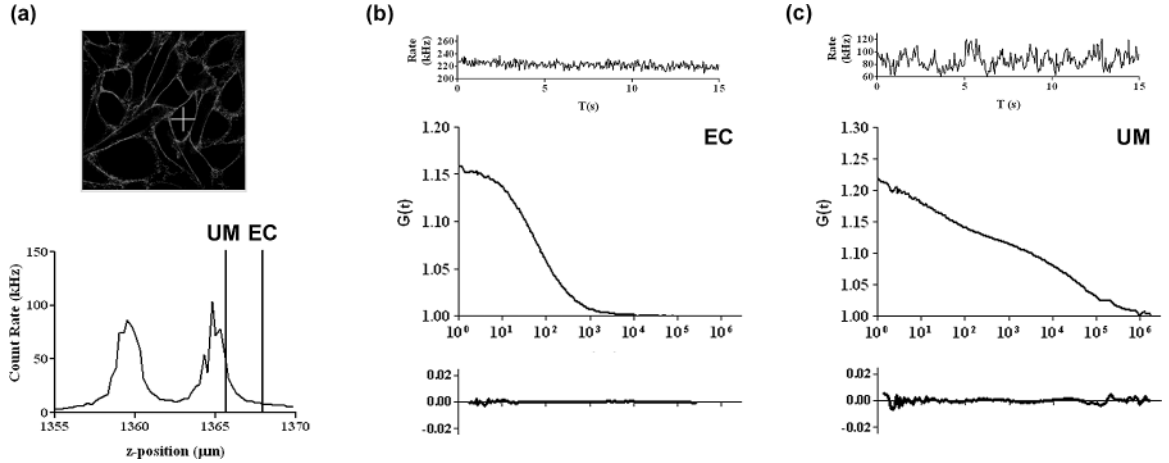

Figure 3. Monitoring binding of **9b** (5 nM) to CHO-A1H cell membranes using FCS. (a) The confocal detection volume was positioned in *x* and *y* using a live epi-fluorescent image of the cells (white cross). Intensity scanning in *z* allowed positioning of the volume on (UM) or 2 μm above (EC) the intensity peaks corresponding to the upper cell membrane. (b) Fluorescence fluctuations detected in the EC position and their subsequent autocorrelation analysis. Curve fitting indicated these data to show a monophasic decay curve with $\tau_{D1} = 60$ μs (100%). Residuals of the fit are shown in the lower graph. (c) Equivalent analysis with data collected on the UM position. The curve was best fit with a three component model showing $\tau_{D1} = 60$ μs (35%), $\tau_{D2} = 8.6$ ms (35%), and $\tau_{D3} = 109$ ms (30%). Data are from an individual cell representative of (b) 16 and (c) 47 experiments performed.

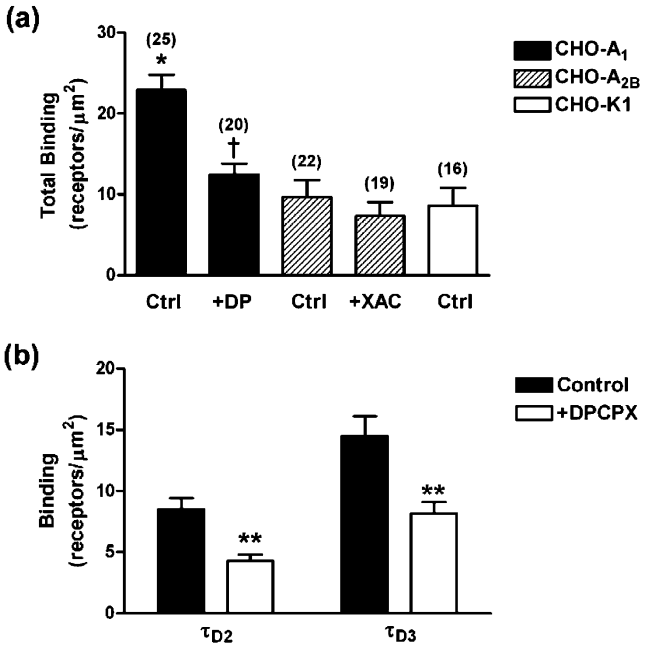

Figure 4. Quantifying binding of **9b** to CHO cell membranes using FCS. (a) CHO-A1H, CHO-A2B, or native CHO-K1 cells were incubated with **9b** (5 nM, 10 min) in the absence (Ctrl) or following a 30 min preincubation with antagonist (100 nM DPCPX (+DP) for CHO-A1H cells; 1 μM XAC (+XAC) for CHO-A2B cells). FCS measurements were then taken on the upper cell membrane, and the total binding was quantified. Results are presented as mean ± s.e. mean, with the number of cells indicated above the column in parenthesis. $^{*}P < 0.001$ vs CHO-K1 binding $^{\dagger}P < 0.001$ vs control for CHO-A1H cells. (b) The results from CHO-A1H cells in (a), indicating the relative levels of the τ_{D2} and τ_{D3} components and their sensitivity to preincubation with DPCPX. $^{**}P < 0.01$ vs control.

Conclusions

We have successfully synthesized and characterized five new red-emitting fluorescent agonists, **9a**−**d** and **14**, for the human adenosine A_1-receptor (A_1-AR). Installation of a range of alkylamine linkers at the N^6-position of either adenosine or NECA generated a range of fully deprotected congeners, functionally equipped to undergo a high yielding chemoselective acylation with the commercially available fluorochrome BODIPY 630/650-X, SE (Molecular Probes). No protecting group manipulations were required following installation of the fluorophore thereby obviating any deleterious side-reactions or loss of yield that may result from the often harsh deprotection conditions employed in chemical synthesis. Mindful of the potential effects the fluorophore may exert on the interactions of these ligands with the A_1-AR, coupled with the fact that the binding site for adenosine is buried within the transmembrane domain of the GPCR, an evaluation of the pharmacology of the new fluorescent derivatives was undertaken. All of the molecules displayed potent agonist activity, despite a tripling of molecular weight when compared to the native receptor agonist. We were further able to utilize these molecules to visualize ligand−receptor interactions using confocal microscopy. Incubation of CHO cells expressing the A_1-AR with the fluorescent agonists resulted in clear labeling of the cell membrane, with a large proportion of this binding prevented by preincubation with a nonfluorescent A_1-AR antagonist, DPCPX. The highest level of membrane binding was displayed by the modified NECA ligands containing a four- or five-carbon linker. Specific labeling of the A_1-AR was further confirmed using a CHO cell line expressing a *C*-terminal GFP-fused A_1-AR. In this example, clear membrane binding of **9b** was observed, which co-localized with the membrane fraction of the fluorescent receptor. Quantification of agonist binding in a small (~0.1 μm^2) area of cell membrane was achieved using the noninvasive technique of FCS. This revealed the existence of at least two types of agonist−receptor complexes with differing diffusion characteristics. Further investigations will concentrate on identifying the nature of these complexes, which may give us further insight into the macrostructure of the A_1-AR and its associated signaling molecules. It will allow us to localize these measurements to specific membrane domains and determine the pharmacology of the A_1-AR subpopulations within them.

Experimental Section

General Chemistry Methods: Chemicals and solvents (HPLC grade) were purchased from the standard suppliers and were used without further purification. BODIPY fluorophores were obtained from Molecular Probes, Cambridge Bioscience, Cambridge, U.K. Merck Kieselgel 60, 230−400 mesh, for flash chromatography was

supplied by Merck KgaA (Darmstadt, Germany), and deuterated solvents were purchased from Goss International Limited (England). Unless otherwise stated, reactions were carried out at ambient temperature. Reactions were monitored by TLC on commercially available precoated aluminum-backed plates (Merck Kieselgel 60 F_{254}). Visualization was by examination under UV light (254 and 366 nm). General staining employed $KMnO_4$. A solution of ninhydrin (EtOH) was used for the visualization of primary amines. All organic extracts collected after aqueous workup procedures were dried over anhydrous magnesium sulfate, filtered under gravity, and evaporated to dryness. Organic solvents were evaporated in vacuo at a temperature of <35 °C (water bath). Purification using preparative layer chromatography was carried out using Fluka silica gel GF_{254} on glass plates (200 mm × 200 mm × 1 mm).

Melting points were recorded on a Gallenkamp 3A 3790 apparatus and are uncorrected. FT-infrared spectra were recorded as thin films or KBr discs in the range of 4000−600 cm^{-1} using an Avatar 360 Nicolet FT-IR spectrophotometer. Optical rotation was measured on a Bellingham-Stanley ADP220 polarimeter. Lyophilization, from either water or 1,4-dioxane, was carried out on an Edwards Modulyo FD freeze drier. Mass spectra (±ES/AP) were recorded by Dr Cath Ortori, School of Pharmacy, University of Nottingham, on a Micromass Platform instrument, using either direct injection or liquid chromatography−mass spectrometry (LC-MS). HRMS TOF-ES mass spectra were recorded on a Waters 2795 Separation Module/Micromass LCT platform. Microanalytical data were recorded by Mr. T. Spencer, School of Chemistry, University of Nottingham. Proton nuclear magnetic resonance spectra were recorded on a Bruker-AMX 250 (250 MHz) or a Bruker-AV 400 (400 MHz) spectrometer. Carbon nuclear magnetic resonance spectra were recorded at 62.9 and 100.6 MHz, respectively. Unless otherwise stated, spectra were recorded in $CDCl_3$. Chemical shifts (δ) are recorded in ppm with reference to the chemical shift of the deuterated solvent/an internal tetramethylsilane standard. Coupling constants (*J*) are recorded in hertz, and the signal multiplicities are described by the following: s, singlet; d, doublet; t, triplet; q, quartet; br, broad; m, multiplet; dd, doublet of doublets. Spectra were assigned using appropriate COSY, DEPT, and HMQC sequences. Analytical reverse-phase high performance liquid chromatography (RP-HPLC) was performed on a Waters Millennium 995 LC system using columns, gradients, and flow rates as described. The eluent was monitored using photodiode array detection. Mobile phases were solvent A, water, and solvent B, acetonitrile, degassed by helium bubble and sonication, respectively.

2′,3′-Isopropylideneinosine (2): Inosine (5.36 g, 0.02 mol) and tosic acid monohydrate (3.80 g, 0.02 mol) were suspended in a mixture of 2,2-dimethoxypropane (50 mL) and acetone (200 mL) and stirred for 18 h. Sodium hydrogen carbonate (2.52 g, 0.02 mol) and water (40 mL) were added, and the suspension was stirred for 15 min. The suspension was evaporated to constant volume, and the crude product was recrystallized from the residual water, yielding the acetonide **2** (3.71 g, 60%) as white needles: mp 266−268 °C (lit. 266 °C;[24] 267 °C[25]); $[\alpha]_D^{22}$ −67.1 (*c* 0.59 in MeOH) (lit. $[\alpha]_D^{20}$ −66.9 (*c* 0.8 in MeOH[25])); δ_H (400 MHz, DMSO-d_6) 1.32 (3H, s, CH_3), 1.54 (3H, s, CH_3), 3.56 (2H, m, $C^{5'}H_2$), 4.23 (1H, m, $C^{4'}H$), 4.93 (1H, dd, J = 6.1, 2.4, $C^{3'}H$), 5.26 (1H, dd, J = 6.1, 2.9, $C^{2'}H$), 6.10 (1H, d, J = 2.9, $C^{1'}H$), 8.09 (1H, s, adenine CH), 8.30 (1H, s, adenine CH), 12.53 (1H, br s, NH); δ_C (100.2 MHz, DMSO-d_6) 25.1, 26.9 (2 × CH_3), 61.4 (CH_2), 81.2, 83.7, 86.6, 89.6 ($C^{1'}$, $C^{2'}$, $C^{3'}$, $C^{4'}$), 113.0 (ketal 4°), 125.4 (4°), 138.7 (adenine CH), 146.0 (adenine CH), 147.7 (4°), 156.5 (C═O); *m*/*z* (ES^+) 309 $(MH)^+$, 137 $(M-ribose)^+$.

2′,3′-Isopropylidene-5′-oxoinosine (3): Acetonide **2** (3.08 g, 10 mmol), TEMPO (313 mg, 2 mmol), and iodosobenzene diacetate (7.09 g, 22 mmol) were dissolved in MeCN/H_2O (1:1, 50 mL) and stirred, with the exclusion of light, for 4 h. The solvents were carefully evaporated from the resultant suspension, and the reaction residue was sequentially triturated with acetone and diethyl ether to yield the acid **3** (2.67 g, 83%) as a white powder: mp 224−229 °C (lit. 272−274 °C;[13a] 252 °C[26]); $[\alpha]_D^{25}$ −59.1 (*c* 0.66 in 1 M NaOH); δ_H (400 MHz, DMSO-d_6) 1.34 (3H, s, CH_3), 1.52 (3H, s, CH_3), 4.67 (1H, d, J = 1.7, $C^{4'}H$) 5.36−5.42 (2H, m, $C^{2'}H$ and $C^{3'}H$), 6.29 (1H, s, $C^{1'}H$), 8.02 (1H, s, adenine CH), 8.29 (1H, s, adenine CH), 12.41 (1H, br s, NH); δ_C (100.2 MHz, DMSO-d_6) 25.3, 26.9 (2 × CH_3), 84.0, 84.2 ($C^{2'}$, $C^{3'}$), 85.9 ($C^{4'}$), 90.1 ($C^{1'}$), 113.1 (ketal 4°), 124.7 (4°), 140.3 (adenine CH), 145.8 (adenine CH), 148.5 (4°), 157.7 (4°), 171.2 (COOH); Anal. ($C_{13}H_{14}N_4O_6$) C, H, N; *m*/*z* (ES^+) 323 $(MH)^+$, 137 $(M-ribose)^+$.

6-Chloro-6-deoxy-5′-ethylamino-2′,3′-isopropylidene-5′-oxo-5′-deoxyinosine (4): Under rigorously dry conditions and an inert atmosphere, acid **3** (967 mg, 3 mmol) was suspended in $CHCl_3$ (15 mL) to which was added *N*,*N*-DMF (581 μL, 7.5 mmol) and $SOCl_2$ (1.09 mL, 15 mmol). The suspension was placed in a hot oil bath and maintained at a gentle reflux for 5 h. The resultant solution was evaporated, and the yellow oil was dissolved in THF (20 mL) at 5 °C. Ethylamine (2.0 M solution in THF, 3.75 mL, 7.5 mmol) was added dropwise, stirred at 5 °C for 15 min, and allowed to warm to room temperature. The solvent was evaporated, and the residue was dissolved in DCM (25 mL) and washed with water (2 × 20 mL) and saturated brine solution (2 × 20 mL). The organic fraction was dried and evaporated to leave a yellow solid that was purified by column chromatography on silica (5% MeOH−DCM) to give the title compound **4** (941 mg, 85%) as a yellow solid: mp 94−96 °C; $[\alpha]_D^{19}$ −12.9 (*c* 0.50 in $CHCl_3$); δ_H (400 MHz) 0.80 (3H, t, J = 7.3, CH_2CH_3), 1.41 (3H, s, CH_3), 1.64 (3H, s, CH_3), 2.90−3.10 (2H, m, CH_2CH_3), 4.74 (1H, d, J = 2.0, $C^{4'}H$), 5.45 (1H, dd, J = 6.2, 2.3, $C^{2'}H$), 5.54 (1H, dd, J = 6.2, 2.0, $C^{3'}H$), 6.23 (1H, d, J = 2.3, $C^{1'}H$), 8.25 (1H, s, adenine CH), 8.75 (1H, s, adenine CH); δ_C (100.2 MHz) 14.2 (CH_2CH_3), 25.0, 26.9 (2 × CH_3), 33.9 (CH_2CH_3), 82.9, 83.4 ($C^{2'}$, $C^{3'}$), 86.7 ($C^{4'}$), 92.0 ($C^{1'}$), 114.1 (ketal 4°), 132.3 (4°), 144.7 (adenine CH), 150.9 (4°), 151.9 (4°), 152.2 (adenine CH), 168.1 (C═O); *m*/*z* (ES^-) 366 $(M-H)^-$, 153 $(M-ribose)^-$; *m*/*z* HRMS (TOF ES^+) $C_{15}H_{19}ClN_5O_4$ $(MH)^+$ calcd, 368.1126; found, 368.1104.

***N*^{1}-Benzyloxycarbonyl-1,*n*-alkyldiamines (*n* = 3, 4, 5, 8; 5a−d):**[27] A solution of benzyl chloroformate (1 equiv) in $CHCl_3$ was added dropwise (3 h) to a stirred solution of 1,*n*-diaminoalkane (5−10 equiv) in $CHCl_3$ at 0 °C. The reaction was allowed to warm to room temperature and stirred for 18 h. The reaction was concentrated, and the residue was partitioned between EtOAc and water. The organic layer was washed with water (×3), and the combined aqueous phases were discarded. The organic layer was washed with 2 M $HCl_{(aq)}$ (×3), and the aqueous layers were combined, adjusted to pH 12 (NaOH), and saturated with NaCl. Following extraction with EtOAc (×3), the combined organic fractions were washed with brine (×2), dried, and evaporated to yield the title compounds **5a**−**d** (35−65%), which were used without further purification.

***N*^{1}-Benzyloxycarbonyl-1,4-butanediamine (5b):**[28] A pale yellow wax; δ_H (250 MHz) 1.48−1.33 (6H, m, C^2H_2, C^3H_2, NH_2), 2.65 (2H, t, J = 6.0, C^4H_2), 3.14 (2H, q, J = 6.0, C^1H_2), 5.06 (2H, s, benzyl CH_2), 5.74 (1H, s, carbamate NH), 7.31 (5H, s, aromatics); δ_C (69.2 MHz) 27.3 (CH_2), 30.7 (CH_2), 41.4 (CH_2, C^4), 41.7 (CH_2, C^1), 66.3 (benzyl CH_2), 128.0 (CH), 128.4 (CH), 136.8 (4°, ipso), 156.6 (4°, C═O); *m*/*z* (ES^+) 223 $(MH)^+$; FT−IR (thin film) 3327, 3031, 2935, 2864, 1686, 1537, 1454, 1254, and 1027 cm^{-1}.

***N*^{6}-(4-Benzyloxycarbonylaminobutyl)-5′-ethylamino-2′,3′-isopropylidene-5′-oxo-5′-deoxyadenosine (6b):** Chloride **4** (300 mg, 0.82 mmol) was dissolved in ethanol (15 mL) to which **5b** (503 mg, 2.46 mmol) and DIEA (0.17 mL, 0.98 mmol) was added. The solution was maintained at reflux under an inert atmosphere for 20 h. The reaction mixture was concentrated, and the residue was purified by column chromatography (10% MeOH−DCM) to yield **6b** (125 mg, 69%) as a colorless oil/foam: δ_H (400 MHz) 0.80 (3H, t, J = 7.2, CH_2CH_3), 1.31 (3H, s, CH_3), 1.55 (3H, s, CH_3), 1.58−1.66 (4H, m, 2 × CH_2), 3.03 (2H, m, CH_2CH_3), 3.19 (2H, m, CH_2), 3.58 (2H, m, CH_2) 4.62 (1H, d, J = 1.3, $C^{4'}H$), 5.02 (2H, s, benzyl CH_2), 5.25 (2H, m, $C^{2'}H$ and $C^{3'}H$), 5.95 (1H, s, $C^{1'}H$), 6.25 (1H, br s, NH), 7.07 (1H, br s, NH), 7.20 (5H, m, phenyl CH), 7.72 (1H, s, adenine CH), 8.24 (1H, s, adenine CH); δ_c (100.2 MHz) 14.3 (CH_2CH_3), 25.1, 26.9 (2 × CH_3), 27.1 (2 × CH_2), 33.9 (CH_2CH_3), 40.0, 40.5 (2 × CH_2), 66.7 (benzyl CH_2), 82.4, 83.6

($C^{2'}$, $C^{3'}$), 85.7 ($C^{4'}$), 92.0 ($C^{1'}$), 114.5 (4°), 128.1 (4°), 128.5 (4°), 136.6 (4°), 139.2 (adenine CH), 153.3 (4°), 155.1 (4°), 156.6 (adenine CH), 168.7 (C═O); *m/z* HRMS (TOF ES$^+$) $C_{27}H_{35}N_7O_6$ $(MH)^+$ calcd, 554.2728; found, 554.2765.

***N*^{6}-(4-Benzyloxycarbonylaminobutyl)-5′-ethylamino-5′-oxo-5′-deoxyadenosine (7b):** Adenosine derivative **6b** (261 mg, 0.47 mmol) was dissolved in 2 M $HCl_{(aq)}$/1,4-dioxane (1:1, 4 mL), placed in a 70 °C oil bath, and stirred for 1 h. The resultant solution was adjusted to ∼pH 8 (satd $NaHCO_{3(aq)}$), saturated with NaCl, and extracted with EtOAc (3 × 5 mL). The combined organic fractions were dried and evaporated, and the crude product was purified by preparative layer chromatography (10% MeOH−DCM) to give the title compound **7b** (160 mg, 66%) as a white solid; mp 90−91 °C (MeOH); δ_H (250 MHz, DMSO-d_6) 1.08 (3H, t, J = 7.2, CH_2CH_3), 1.45−1.62 (4H, m, 2 × CH_2), 3.02 (2H, app q, CH_2) 3.22 (2H, app quintet, CH_2CH_3), 3.40−3.55 (2H, m, CH_2), 4.14 (1H, m, $C^{3'}H$), 4.31 (1H, d, J = 1.1, $C^{4'}H$), 4.61 (1H, m, $C^{2'}H$), 4.99 (2H, s, benzyl CH_2), 5.56 (1H, d, J = 6.5, $C^{2'}$-OH), 5.76 (1H, d, J = 4.2, $C^{2'}$-OH), 5.96 (1H, d J = 7.6, $C^{1'}H$), 7.26−7.34 (6H, m, phenyl CH and carbamate NH), 8.01 (1H, br s, NH), 8.27 (1H, s, adenine CH), 8.39 (1H, s, adenine CH), 8.94 (1H, t, J = 5.6, amide NH); δ_c (69.2 MHz, DMSO-d_6) 14.9 (CH_2CH_3), 26.6, 27.1 (2 × CH_2), 33.4 (CH_2CH_3), 39.5, 40.3 (2 × CH_2), 65.3 (benzyl CH_2), 72.2 ($C^{2'}$), 73.3 ($C^{3'}$), 84.9 ($C^{4'}$), 88.0 ($C^{1'}$), 120.2 (4°), 127.9 (4°), 128.5 (phenyl CH), 137.5 (adenine CH), 140.6 (4°), 148.4 (4°), 152.3 (adenine CH), 154.9 (4°), 156.3 (4°), 169.3 (amide C═O); *m/z* HRMS (TOF ES$^+$) $C_{24}H_{31}N_7O_6$ $(MH)^+$ calcd, 514.2415; found, 514.2371.

***N*^{6}-(Aminoalkyl)-5′-ethylamino-5′-oxo-5′-deoxyadenosines (8a−d):** Adenosine derivatives **7a−d** (50 mg) were dissolved in MeOH/H_2O/AcOH (9:0.9:0.1, 5 mL), to which was added 10% Pd/C (10 mg). The flask was evacuated, filled with hydrogen (balloon), and stirred vigorously for 2−3 h. The reaction mixture was filtered through celite, and the celite was washed with MeOH. The combined organic filtrates were evaporated, and the resultant oil was evaporated again from MeCN (2 × 15 mL) to give the title compounds **8a−d** (quantitative) as colorless oils/foams.

***N*^{6}-(4-Aminobutyl)-5′-ethylamino-5′-oxo-5′-deoxyadenosine (ABEA; 8b):** δ_H (400 MHz, MeOH-d_4) 1.20 (3H, t, J = 7.3, CH_2CH_3), 1.75−1.81 (4H, m, 2 × CH_2), 2.96−3.03 (2H, m, CH_2), 3.36 (2H, q, J = 7.3, CH_2CH_3), 3.66 (2H, m, CH_2), 4.31 (1H, dd, J = 1.3, 4.7, $C^{3'}H$), 4.47 (1H, d, J = 1.3, $C^{4'}H$), 4.74 (1H, dd, J = 4.8, 7.6, $C^{2'}H$), 6.01 (1H, d, J = 7.7, $C^{1'}H$), 8.27 (2H, s, adenine CH); δ_C (100.2 MHz, MeOH-d_4) 15.1 (ethyl CH_3), 22.6 (CH_2), 25.9 (CH_2), 27.6 (CH_2), 35.1 (CH_2), 40.4 (CH_2), 73.5 (CH), 75.0 (CH), 86.4 (CH), 90.4 (CH), 121.7 (4°), 142.4 (CH), 149.3 (4°), 153.7 (CH), 156.4 (4°), 172.1 (4°); *m/z* HRMS (TOF ES$^+$) $C_{16}H_{25}N_7O_4$ $(M + H)^+$ calcd, 380.2047; found, 380.2032.

Conjugation with BODIPY 630/650-X, SE: Ligands **8a−d** (15.1 μmol) were dissolved in *N*,*N*-DMF (1.0 mL) under an inert atmosphere and with the exclusion of light. A solution of BODIPY 630/650-X, SE (Molecular Probes; 5.0 mg, 7.55 μmmol, 1 mL *N*,*N*-DMF) was added, and the reaction was stirred for 4 h. The solution was evaporated, and the crude product was purified by preparative layer chromatography (10% MeOH−DCM) to give the title compound **9a−d** as purple powders (75−85%). When submitted to analytical HPLC (Jones C^8 column, [250 mm × 4.6 mm], 1 mL·min^{-1}, 35−100% B, 30 min, monitored using photodiode array detection between 190 and 800 nm; mobile phases; solvent A, H_2O; solvent B, MeCN), all probes were observed to elute as single and symmetrical peaks at the retention time R_t given below for each compound. The purity of the ligands was confirmed by performing a second analytical HPLC (Jones C^4 column, [250 mm × 4.6 mm], 1 mL·min^{-1}, 35−100% B, 30 min, monitored using photodiode array detection between 190 and 800 nm; mobile phases; solvent A, H_2O; solvent B, MeCN). Again, all target compounds eluted as homogeneous single peaks. The identities of the compounds were further analyzed by HRMS (TOF ES$^+$).

(2*S*,3*S*,4*R*,5*R*,*E*)-*N*-Ethyl-3,4-dihydroxy-5-(6-(4-(6-(2-(4-(2-(4,4-difluoro-4,4a-dihydro-5-(thiophen-2-yl)-4-bora-3a,4a-diaza-*s*-indacene-3-yl)vinyl)phenoxy)acetamido)hexanamido)butylamino)-9*H*-purin-9-yl)-tetrahydrofuran-2-carboxamide (9b): δ_H (400 MHz, DMSO-d_6) 1.08, (3H, t, J 7.2, ethyl CH_3), 1.19−1.26 (2H, m, CH_2), 1.40−1.62 (8H, m, 4 × CH_2), 2.03 (2H, t, J = 7.4, CH_2), 3.02−3.27 (6H, m, 2 × CH_2, ethyl CH_2), 3.48 (2H, m, CH_2), 4.12−4.16 (1H, m, $C^{3'}H$), 4.31 (1H, d, J = 1.4, $C^{4'}H$), 4.54 (2H, s, BODIPY CH_2), 4.59−4.64 (1H, m, $C^{2'}H$), 5.54 (1H, d, J = 6.5, $C^{2'}$-OH), 5.74 (1H, d, J = 4.2, $C^{3'}$-OH), 5.97 (1H, d, J = 7.8, $C^{1'}H$), 6.96 (1H, d, J = 4.2), 7.08 (2H, d, J = 8.8), 7.27−7.30 (3H, m), 7.38 (1H, d, J = 4.4), 7.42 (1H, br s), 7.61 (1H, s), 7.62 (2H, d, J = 8.7), 7.72−7.76 (2H, m), 7.83 (1H, dd, J = 5.0, 0.9), 7.94−8.01 (1H, m), 8.04 (1H, dd, J = 3.8, 0.9), 8.12 (1H, t, J = 5.7), 8.27 (1H, br s), 8.39 (1H, s, adenine CH), 8.91 (1H, t, J = 5.6, amide NH); R_t 13.61 min (Jones C^8, 250 × 4.6 mm, 1 mL·min^{-1}, 35−100% B, 30 min), R_t-2 9.31 min (Jones C^4, 250 × 4.6 mm, 1 mL·min^{-1}, 35−100% B, 30 min; solvent A, H_2O; solvent B, MeCN); *m/z* HRMS (TOF ES$^+$) $C_{45}H_{51}BF_2N_{10}O_7S$ $(MH)^+$ calcd, 925.3803; found, 925.3842.

2′,3′,5′-Tri-*O*-acetylinosine (10): a solution of inosine (5.16 g, 19 mmol), pyridine (50 mL), and acetic anhydride (50 mL) was heated at 50 °C for 12 h. Upon cooling, the solution was filtered, and the filtrate was evaporated under high vacuum to leave a pale yellow solid. The solid was triturated with diethyl ether and filtered to yield the crude product as a white solid (7.37 g). Recrystallization from methanol (150 mL) yielded the title compound **10** as a white crystalline solid (6.11 g, 80%): mp 235 °C, MeOH (lit.[30] 241 °C); $[\alpha]_D^{24}$ −26.0 (*c* 1.0, MeOH) (lit.[29] $[\alpha]_D^{20}$ −36.5 ($CHCl_3$)); δ_H (250 MHz) 2.10 (3H, s, OAc), 2.15 (3H, s, OAc), 2.16 (3H, s, OAc), 4.36−4.47 (3H, m, $C^{4'}H$, $C^{5'}H$), 5.54 (1H, t, J = 5.4, $C^{3'}H$), 5.90 (1H, t, J = 5.6, $C^{2'}H$), 6.18 (1H, d, J = 5.5, $C^{1'}H$), 8.03 (1H, s, C^8H), 8.32 (1H, s, C^2H), 13.09 (1H, s, NH); δ_C (69.2 MHz) 20.4, 20.6, 20.8 (3 × OAc), 63.0 ($C^{5'}$), 70.6, 73.4, 80.4 ($C^{2'}$, $C^{3'}$, $C^{4'}$), 86.5 ($C^{1'}$), 125.4 (4°), 138.6, 145.8 ($C^{2'}$, $C^{8'}$), 148.8 (4°), 159.0 (4°), 169.3, 169.6, 170.4 (3 × CO); FT−IR (KBr) 1748, 1702, 1588, 1376, 1227, 1053 cm^{-1}; *m/z* (ES$^+$) 395 $(MH)^+$.

2′,3′,5′-Tri-*O*-acetyl-6-chloroinosine (11): A suspension of **10** (2.45 g, 6.22 mmol), *N*,*N*-dimethylaniline (0.83 mL, 6.53 mmol), and phosphorus oxychloride (12.2 mL, 131 mmol) was stirred at room temperature for 7 min under an atmosphere of nitrogen. The flask was heated in a preheated oil bath and maintained at reflux for 13 min. The solution was evaporated, and the resulting oil was stirred in chloroform (20 mL) and ice (∼20 mL). The aqueous layer was extracted with chloroform (2 × 25 mL). The combined organic layers were washed with 2 M HCl (4 × 20 mL) and brine (2 × 20 mL), dried, and evaporated to yield 3 g of green oil. Purification using silica chromatography (1:9 MeOH/DCM) yielded the title compound **11** as a pale brown viscous oil (2.18 g, 85%): $[\alpha]_D^{24}$ −18.5 (c 1.3, MeOH); δ_H (250 MHz) 2.10 (3H, s, OAc), 2.13 (3H, s, OAc), 2.17 (3H, s, OAc), 4.36−4.54 (3H, m, $C^{4'}H$, $C^{5'}H$), 5.67 (1H, t, J = 5.2, $C^{3'}H$), 5.97 (1H, t, J = 5.3, $C^{2'}H$), 6.27 (1H, d, J = 5.5, $C^{1'}H$), 8.37 (1H, s, adenine CH), 8.79 (1H, s, adenine CH); δ_C (69.2 MHz) 20.1, 20.5, 20.8 (3 × OAc), 62.9 ($C^{5'}$), 70.5, 73.1, 80.5, 86.9 ($C^{1'}$, $C^{2'}$, $C^{3'}$, $C^{4'}$), 132.3 (4°), 143.7 (adenine CH), 151.3 (4°), 151.6 (4°), 152.3 (adenine CH), 169.4, 169.6, 170.3 (3 × CO); FT−IR (thin film) 1747, 1588, 1564, 1376, 1225, 1049 cm^{-1}; *m/z* (ES$^+$) 413 $(MH)^+$, 259 $(M-purine)^+$.

***N*^{6}-(Benzyloxycarbonylaminobutyl)adenosine (12):** A solution of chloride **11** (1.13 g, 2.7 mmol), diamine **5b** (2.42 g, 10.9 mmol), and DIEA (0.47 mL, 2.7 mmol) was refluxed in EtOH (40 mL) for 18 h. The solution was evaporated, and the residue was dissolved in an ice-cold, saturated methanolic solution of NH_3. The solution was stirred at 0 °C for 2 h, warmed to room temperature, and stirred for an additional 2 h. The MeOH was evaporated to yield a solid. Purification by silica chromatography (1:9 MeOH/DCM) yielded 1 g of yellow solid. Recrystallization from EtOH (30 mL) gave the title compound **12** as a white solid (742 mg, 58%): mp 134 °C, EtOH; $[\alpha]_D^{24}$ −48.0 (*c* 1.0, MeOH/water, 4:1); δ_H (250 MHz, DMSO-d_6) 1.40−1.60 (4H, m, 2 × CH_2), 3.02 (2H, m, CH_2), 3.37−3.79 (4H, m, CH_2, $C^{5'}H$), 3.97 (1H, m, $C^{4'}H$), 4.15 (1H, m, $C^{3'}H$), 4.62 (1H, m, $C^{2'}H$), 5.00 (2H, s, benzylic CH_2), 5.22 (1H, d, J 4.5, OH, exchanges D_2O), 5.47 (2H, m, carbamate NH, OH, exchanges D_2O), 5.98 (1H, d, J = 6.1, $C^{1'}H$), 7.34 (5H, s, aromatics), 7.95 (1H, br s, NH, exchanges D_2O), 8.21 (1H, s, purine C^2H), 8.35

(1H, s, purine C^8H); δ_C (69.2 MHz, DMSO-d_6) 26.6 (CH_2), 27.1 (CH_2), 39.5 (CH_2), 41.0 (CH_2), 61.9 (CH_2, $C^{5'}$), 65.3 (CH_2, benzylic), 70.9 (CH), 73.7 (CH), 86.1 (CH), 88.2 (CH), 120.0 (purine C^5), 127.9 (CH, aromatic), 128.5 (CH, aromatic), 137.5 (4°, ipso), 139.9 (purine C^8), 148.0 (purine C^6), 152.6 (purine C^2), 154.9 (purine C^4), 156.3 (carbamate C═O); *m/z* (ES^+) 473 $(MH)^+$, 342 $(M-ribose)^+$; Anal. ($C_{22}H_{28}O_6N_6 \cdot 0.5H_2O$) C, H, N.

***N*^{6}-(Aminobutyl)adenosine (13):** A suspension of **12** (250 mg, 0.53 mmol) and 50 mg of 10% Pd/C in 20 mL of solvent (9:1 MeOH/H_2O with 1% AcOH) was stirred under hydrogen (balloon) for 3 h. The reaction was filtered through a celite pad and was concentrated in vacuo to yield **13** as a colorless oil. Under high vacuum, the oil formed a white hygroscopic solid (219 mg, quantitative): $[\alpha]_D^{24}$ −21.0 (*c* 1.0, MeOH); δ_H (250 MHz, DMSO-d_6) 1.48−1.62 (4H, m, CH_2), 1.79 (5H, br s, OH and NH_2, reduces D_2O), 2.71 (2H, br t, CH_2), 3.41 (2H, br s, CH_2), 3.54 (1H, dd, J = 12.0, 3.5, $C^{5'a}H$), 3.67 (1H, dd, J = 12.0, 3.5, $C^{5'b}H$), 3.97 (1H, m, $C^{4'}H$), 4.16 (1H, m, $C^{3'}H$), 4.62 (1H, t, J = 5.2, $C^{2'}H$), 5.90 (1H, d, J = 6.1, $C^{1'}H$), 7.95 (1H, br s, NH, exchanges D_2O), 8.22 (1H, s, purine C^2H), 8.38 (1H, s, purine C^8H); δ_C (69.2 MHz, DMSO-d_6) 27.2 (CH_2, br), 41.0 (CH_2, br), 61.5 (CH_2, $C^{5'}$), 70.5 (CH), 73.5 (CH), 85.8 (CH), 87.8 (CH), 120.0 (purine C^5), 139.5 (purine C^8), 148.0 (purine C^6), 152.2 (purine C^2), 154.5 (purine C^4); *m/z* HRMS (FAB) $C_{14}H_{23}N_6O_4$ $(MH)^+$ calcd, 339.1781; found, 339.1797.

***N*-(4-(9-((2*R*,3*R*,4*S*,5*R*)-3,4-Dihydroxy-5-(hydroxymethyl)-tetrahydrofuran-2-yl)-9*H*-purin-6-ylamino)butyl)-6-(2-(2-(4,4-difluoro-4,4a-dihydro-5-(thiophen-2-yl)-4-bora-3a,4a-diaza-*s*-indacene-3-yl)vinyl)phenoxy)acetamido)hexanamide (14):** A solution of ABA 13 (4.9 mg, 14.5 μmol) and BODIPY 630/650-X, SE (5 mg, 7.6 μmol) was stirred in *N*,*N*-DMF (1 mL) in the dark, under a nitrogen atmosphere, for 5 h. The DMF was removed in vacuo, and the dark blue residue was purified by preparative layer chromatography (15:85, MeOH/$CHCl_3$) to yield the title compound **14** as a blue solid (5.0 mg, 75%). When submitted to analytical HPLC (Jones C^8 column, [250 mm × 4.6 mm], 1 mL·min^{-1}, 35−100% B, 30 min, monitored using photodiode array detection between 190 and 800 nm; mobile phases; solvent A, H_2O; solvent B, MeCN), **14** was observed to elute as a single and symmetrical peak at retention time R_t given below. The purity of **14** was confirmed by performing a second analytical HPLC (Jones C^4 column, [250 mm × 4.6 mm], 1 mL·min^{-1}, 35%−100% B, 30 min, monitored using photodiode array detection between 190 and 800 nm; mobile phases; solvent A, H_2O; solvent B, MeOH). Again, **14** eluted as a homogeneous single peak. The identity of **14** was further analyzed by ^1H NMR and HRMS (TOF ES^+): δ_H (250 MHz, DMSO-d_6) 1.69−1.15 (11H, m), 2.00 (2H, m), 3.21−3.0 (4H, m), 3.70−3.45 (3H, m), 3.97 (1H, m, $C^{4'}H$), 4.16 (1H, m, $C^{3'}H$), 4.54 (2H, s, BODIPY CH_2), 4.62 (1H, q, J = 6.0, $C^{2'}H$), 5.20 (1H, d, J = 4.6), 5.50−5.45 (2H, m), 5.90 (1H, d, J = 6.0, $C^{1'}H$), 6.96 (1H, d, J 4.3) 7.10−7.07 (2H, m), 7.43−7.27 (4H, m), 7.63−7.60 (3H, m), 7.79−7.72 (2H, m), 7.83 (1H, d, J = 3.0), 7.90 (1H, br s), 8.05 (1H, d, J 3.0), 8.22−8.15 (2H, m), 8.38 (1H, s, purine C^8); *m/z* HRMS (FAB) $C_{43}H_{49}BF_2N_9O_7S$ $(MH)^+$ calcd, 884.3538; found, 884.3774; R_t 13.19 min (Jones C^8, 250 × 4.6 mm, 1 mL·min^{-1}, 35−100% B, 30 min), R_t-2 9.13 min (Jones C^4, 250 × 4.6 mm, 1 mL·min^{-1}, 35−100% B, 30 min; solvent A, H_2O; solvent B, MeCN).

General Pharmacology Methods: Measurement of [^{3}H]-cAMP Accumulation: The human adenosine A_3 receptor cDNA, cloned into pcDNA3.1+ (Invitrogen) was obtained from UMR cDNA Resource Center (U.S.A.). This was transfected into CHO-K1 cells (European Collection of Animal Cell Cultures, Porton Down, Salisbury, U.K.) using lipofectamine (according to manufacturer's instructions). Stably transfected CHO-K1 cells (CHO-A3 cells) were selected using 500 μg/mL Geneticin (G418; Life Technologies, Inc., Gaithersburg, MD) for two weeks. CHO-A3 cells resistant to G418 were subsequently cloned by dilution cloning. Clonal CHO-A3 cells, CHO-A1H cells,[20] CHO-A2B cells,[30] or CHO-A2A cells (a gift from Dr. K. N. Klotz, Wurzburg, Germany) were grown in 24-well cluster dishes until confluent. Cells were incubated with 1 mL of Hank's buffered salt solution (Sigma) containing 20 mM HEPES (HHB) and [^{3}H]adenine (Amersham Biosciences, 37 kBq per well) for 2 h at 37 °C. Cells were washed twice with HHB (1 mL) before incubation with the phosphodiesterase inhibitor rolipram (10 μM) for 15 min at 37 °C. Where stated, cells were incubated with the antagonist DPCPX (100 nM). In the case of CHO-A1H and CHO-A3 cells, agonists were added for 5 min, prior to incubation with forskolin (3 μM) for an additional 10 min, in a final volume of 1 mL. For CHO-A2A and CHO-A2B cells, agonists were added for 10 min in the absence of forskolin. Incubations were terminated by the addition of concentrated HCl (50 μL). [^{3}H]-cAMP was isolated by single column alumina chromatography, as previously described,[31] and levels were determined by liquid scintillation counting.

Measurement of [^{3}H]-DPCPX Binding to CHO-A1H Cells. CHO-A1H cells were grown in white-sided 96-well view plates. In saturation studies, once the cells were confluent, 100 μL of serum-free media or serum-free media containing 20 μM XAC (to define nonspecific binding) was added to each well, immediately followed by 100 μL of serum-free media containing a range of [^{3}H]-DPCPX concentrations (0.004−38 nM). For competition studies, the media was removed and replaced with 100 μL serum-free media (i.e., DMEM/F12 containing 2 mM L-glutamine only) containing the competing ligand at twice the final required concentration. Immediately, 100 μL of serum-free media containing [^{3}H]-DPCPX was added to each well (hence, 1:2 dilutions in well) to give final required concentrations. [^{3}H]-DPCPX was used at a concentrations of 1 nM. Total and nonspecific binding (as defined by 10 μM XAC) were measured in every experiment. All plates were incubated for 2 h at 37 °C in a humidified 5% CO_2/95% air atmosphere. After 2 h, media and drugs were removed, and the cells were washed twice with 200 μL of cold PBS/well. A white base was then added to the plate, followed by 100 μL of Microscint 20 per well, and a sealant film was placed over the wells. The plates were then counted the following day on a Topcount (Packard) for 2 min per well at 21 °C. For studies in permeabilized cells, incubation with ligands was performed in serum-free media containing 0.01% Triton-X100 (under these conditions, trypan blue enters all of the cells). At the end of the incubation period, the cells and media from each well were transferred to a 96-well white Millipore Multiscreen HTS FB filter plate, and the cells were collected on the GF-B filter under vacuum. The filters were washed twice with 200 μL of cold PBS/well, and scintillation counting was performed as described above.

Data Analysis: EC_{50}, IC_{50} (concentrations of drug producing 50% of the maximal stimulatory or inhibitory response), and pEC_{50} (negative logarithm of the EC_{50}) values were obtained by computer-assisted curve fitting (to a sigmoidal dose response) using the computer program PRISM (GraphPAD, California). pK_B values were calculated from EC_{50} values obtained in the presence and absence of antagonist using the Gaddum equation:

$$pK_B = \log(\text{concentration ratio} - 1) - \log(\text{antagonist concentration})$$

Saturation curves for specific [^{3}H]-DPCPX binding were fitted to the following equation:

$$\text{Specific binding} = \frac{B_{max} \times K_D}{([L] + K_D)}$$

where B_{max} is the maximum specific binding, K_D is the dissociation constant of [^{3}H]-DPCPX, and [L] is the concentration of [^{3}H]-DPCPX. Curves for inhibition of the binding of [^{3}H]-DPCPX by agonists were fitted to the following equation:

$$\%\text{ of uninhibited binding} = \frac{100 - I_{max}}{1 + ([A]/IC_{50})} + I_{max}$$

where [A] is the concentration of competing ligand, IC_{50} is the

concentration that inhibits the agonist-displaceable binding by 50%, and I_{max} is the maximal inhibition of binding produced by the agonist. Apparent agonist dissociation constants (K_B) were then determined from the following expression:

$$K_B = \frac{IC_{50} \times K_D}{(K_D + [L])}$$

where $[L]$ and K_D are the concentration and dissociation constant of [^{3}H]-DPCPX, respectively, as determined from the saturation binding studies.

Statistical significance was determined by Student's unpaired *t* test, unless otherwise stated. All data are presented as mean ± s.e. mean. The *n* in the text refers to the number of separate experiments performed.

Acknowledgment. We thank Julia A. Weinstein for help with photophysical characterization measurements. This work was supported by The Wellcome Trust (Grant Numbers 057199 and 066817) and The University of Nottingham. The molecules described in this paper are the subject of an international patent application, WO 2004/088312.

Supporting Information Available: Full experimental procedures and compound characterization data for compounds **5**−**9a**,**c**,**d**. Representative spectra for compounds **2**−**9b**. This material is available free of charge via the Internet at http://pubs.acs.org.

References

(1) Ma, P.; Zemmel, R. Value of Novelty? *Nat. Rev. Drug Discovery* **2002**, *1*, 571−572.

(2) Ralevic, V. R.; Burnstock, G. Receptors for Purines and Pyrimidines. *Pharmacol. Rev.* **1998**, *50*, 413−492.

(3) (a) Gines, S.; Ciruela, F.; Burgueno, J.; Casado, V.; Canela, E. I.; Mallol, J.; Lluis, C.; Franco, R. Involvement of Caveolin in Ligand-Induced Recruitment and Internalization of A(1) Adenosine Receptor and Adenosine Deaminase in an Epithelial Cell Line. *Mol. Pharmacol.* **2001**, *59*, 1314−1323. (b) Zajchowski, L. D.; Robbins, S. M. Lipid Rafts and Little Caves−Compartmentalized Signalling in Membrane Microdomains. *Eur. J. Biochem.* **2002**, *269*, 737−752. (c) Helmreich, E. J. M. Environmental Influences on Signal Transduction Through Membranes: A Retrospective Mini-Review. *Biophys. Chem.* **2003**, *100*, 519−534.

(4) (a) Baker, J. G.; Hall, I. P.; Hill, S. J. Pharmacology and Direct Visualisation of BODIPY-TMR-CGP: A Long-Acting Fluorescent Beta(2)-Adrenoceptor Agonist. *Br. J. Pharmacol.* **2003**, *139*, 232−242. (b) Harikumar, K. G.; Pinon, D. I.; Wessels, W. S.; Prendergast, F. G.; Miller, L. J. Environment and Mobility of a Series of Fluorescent Reporters at the Amino Terminus of Structurally Related Peptide Agonists and Antagonists Bound to the Cholecystokinin Receptor. *J. Biol. Chem.* **2002**, *277*, 18552−18560. (c) Emmerson, P. J.; Archer, S.; El-Hamouly, W.; Mansour, A.; Akil, H.; Medzihradsky, F. Synthesis and Characterization of 4,4-Difluoro-4-bora-3a,4a-diaza-*s*-indacene (BODIPY)-Labeled Fluorescent Ligands for the mu Opioid Receptor. *Biochem. Pharmacol.* **1997**, *54*, 1315−1322. (d) Bennett, V. J.; Simmons, M. A. Analysis of Fluorescently Labeled Substance P Analogs: Binding, Imaging, and Receptor Activation. *BMC Chem. Biol.* **2001**, *1*, 1−12.

(5) (a) Schwille, P. Fluorescence Correlation Spectroscopy and its Potential for Intracellular Applications. *Cell Biochem. Biophys.* **2001**, *34*, 383−408. (b) Pramanik, A.; Rigler, R. FCS-Analysis of Ligand−Receptor Interactions in Living Cells. In *Fluorescence Correlation Spectroscopy: Theory and Applications*; Elson, E., Rigler, R., Eds.; Springer: Heidelberg, 2001; pp 101−129.

(6) (a) Bacia, K.; Schwille, P. A Dynamic View of Cellular Processes by In Vivo Fluorescence Auto- and Cross-Correlation Spectroscopy. *Methods* **2003**, *29*, 74−85. (b) Bacia, K.; Scherfeld, D.; Kahya, N.; Schwille, P. Fluorescence Correlation Spectroscopy Relates Rafts in Model and Native Membranes. *Biophys. J.* **2004**, *87*, 1034−1043. (c) Wang, Z.; Shah, J. V.; Chen, Z.; Sun, C. H.; Berns, M. W. Fluorescence Correlation Spectroscopy Investigation of a GFP Mutant-Enhanced Cyan Fluorescent Protein and Its Tubulin Fusion in Living Cells with Two-Photon Excitation. *J. Biomed. Opt.* **2004**, *9*, 395−403. (d) Kim, S. A.; Heinze, K. G.; Waxham, M. N.; Schwille, P. Intracellular Calmodulin Availability Accessed with Two-Photon Cross-Correlation. *Proc. Natl. Acad. Sci. U.S.A.* **2004**, *101*, 105−110. (e) Bacia, K.; Majoul, I. V.; Schwille, P. Probing the Endocytic Pathway in Live Cells Using Dual-Color Fuorescence Cross-Correlation Analysis. *Biophys. J.* **2002**, *83*, 1184−1193.

(7) (a) Weisshart, K.; Jungel, V.; Briddon, S. J. The LSM 510 META ConfoCor 2 System: An Integrated Imaging and Spectroscopic Platform for Single-Molecule Detection. *Curr. Pharm. Biotechnol.* **2004**, *5*, 134−154. (b) Pramanik, A.; Olsson, M.; Langel, U.; Bartfai, T.; Rigler, R. Fluorescence Correlation Spectroscopy Detects Galanin Receptor Diversity on Insulinoma Cells *Biochemistry* **2001**, *40*, 10839−10845. (c) Hegener, O.; Jordan, R.; Haberlein, H. Dye-Labeled Benzodiazepines: Development of Small Ligands for Receptor Binding Studies Using Fluorescence Correlation Spectroscopy *J. Med. Chem.* **2004**, *47*, 3600−3605.

(8) (a) Pramanik, A.; Rigler, R. Ligand−Receptor Interactions in the Membrane of Cultured Cells Monitored by Fluorescence Correlation Spectroscopy. *Biol. Chem.* **2001**, *382*, 371−378. (b) Zhong, Z.-H.; Pramanik, A.; Ekberg, K.; Jansson, O. T.; Jörnvall, H.; Wahren, J.; Rigler, R. Insulin Binding Monitored by Fluorescence Correlation Spectroscopy. *Daibetologia* **2001**, *44*, 1184−1188.

(9) McGrath, J. C.; Arribas, S.; Daly, C. J. Fluorescent Ligands for the Study of Receptors. *Trends Pharmacol. Sci.* **1996**, *17*, 393−399 and references therein.

(10) Briddon, S. J.; Middleton, R. J.; Cordeaux, Y.; Flavin, F. M.; Weinstein, J. A.; George, M. W.; Kellam, B.; Hill, S. J. Quantitative Analysis of the Formation and Diffusion of A(1)-Adenosine Receptor−Antagonist Complexes in Single Living Cells. *Proc. Natl. Acad. Sci. U.S.A.* **2004**, *101*, 4673−4678.

(11) (a) Daly, C. J.; McGrath, J. C. Fluorescent Ligands, Antibodies, and Proteins for the Study of Receptors. *Pharmacol. Ther.* **2003**, *100*, 101−118. (b) Middleton, R. J.; Kellam, B. Fluorophore-Tagged GPCR Ligands. *Curr. Opin. Chem. Biol.* **2005**, *9*, 517−525.

(12) Daly, C. J.; McGrath, J. C. Do Fluorescent Drugs Show You More Than You Wanted To Know? *Br. J. Pharmacol.* **2003**, *139*, 187−189.

(13) (a) Olsson, R. A.; Kusachi, S.; Thompson, R. D.; Ukena, D.; Padgett, W.; Daly, J. W. *N*-6-Substituted *N*-Alkyladenosine-5′-uronamides-bifunctional Ligands Having Recognition Groups for A1 and A2 Adenosine Receptors. *J. Med. Chem.* **1986**, *29*, 1683−1689. (b) Gallo-Rodriguez, C.; Ji, X.-d.; Melman, N.; Siegman, B. D.; Sanders, L. H.; Orlina, J.; Fischer, B.; Pu, Q.; Olah, M. E.; van Galen, P. J. M.; Stiles, G. L.; Jacobsen, K. A. Structure−Activity Relationships of *N*-6-Benzyladenosine-5′-uronamides as A(3)-Selective Adenosine Agonists. *J. Med. Chem.* **1994**, *37*, 636−646. (c) Güngör, T.; Malabre, P.; Teulon, J.-T.; Camborde, F.; Meignen, J.; Hertz, F.; Virone-Oddos, A.; Caussade, F.; Cloarec, A. *N*-6-Substituted Adenosine Receptor Agonists−Synthesis and Pharmacological Activity as Potent Antinociceptive Agents. *J. Med. Chem.* **1994**, *37*, 4307−4316. (d) Ha, S. B.; Nair, V. An Improved Approach to the Synthesis of Adenosine-5′-*N*-ethyluronamides of Interest as Adenosine Receptor Agonists. *Tet. Lett.* **1996**, *37*, 1567−1570. (e) Wright, D. M. J.; Baker, S. P.; Stewart, S. G.; Scammells, P. J. *N*-6-(5,6-Epoxynorbornyl)adenosine Analogs as A(1) Adenosine Agonists. *Bioorg. Med. Chem. Lett.* **1998**, *8*, 3647−3648.

(14) (a) Macchia, M.; Salvetti, F.; Barontini, S.; Calvani, F.; Gesi, M.; Hamdan, M.; Lucacchini, A.; Pellegrini, A.; Soldani, P.; Martini, C. Fluorescent Probes for Adenosine Receptors: Synthesis and Biology of *N*-6-Dansylaminoalkyl-Substituted NECA Derivatives. *Bioorg. Med. Chem. Lett.* **1998**, *8*, 3223−3228. (b) Macchia, M.; Salvetti, F.; Bertini, S.; Di Bussolo, V.; Gattuso, L.; Gesi, M.; Hamdan, M.; Klotz, K.-N.; Laragione, T.; Lucacchini, A.; Minutolo, F.; Nencetti, S.; Papi, C.; Tuscano, D.; Martini, C. 7-Nitrobenzofurazan (NBD) Derivatives of 5′-*N*-Ethylcarboxamidoadenosine (NECA) as New Fluorescent Probes for Human A(3) Adenosine Receptors. *Bioorg. Med. Chem. Lett.* **2001**, *11*, 3023−3026. (c) Jacobson, K. A.; Ukena, D.; Padgett, W.; Kirk, K. L.; Daly, J. W. Molecular Probes for Extracellular Adenosine Receptors. *Biochem. Pharmacol.* **1987**, *36*, 1697−1707.

(15) Epp, J. B.; Widlanski, T. S. Facile Preparation of Nucleoside-5′-carboxylic Acids. *J. Org. Chem.* **1999**, *64*, 293−295.

(16) (a) De Mico, A.; Margarita, R.; Parlanti, L.; Vescovi, A.; Piancatelli, G. A Versatile and Highly Selective Hypervalent Iodine (III)/2,2,6,6-Tetramethyl-1-piperidinyloxyl-Mediated Oxidation of Alcohols to Carbonyl Compounds. *J. Med. Chem.* **1997**, *62*, 6974−6977. (b) de Nooy, A. E. J.; Besemer, A. C.; van Bekkum, H. On the Use of Stable Organic Nitroxyl Radicals for the Oxidation of Primary and Secondary Alcohols. *Synthesis* **1996**, 1153−1174.

(17) (a) Chen, F. M. F.; Benoiton, N. L. Reductive *N*,*N*-Dimethylation of Amino-Acid and Peptide Derivatives Using Methanol as Carbonyl Source. *Can. J. Biochem.* **1978**, *56*, 150−152. (b) Benoiton, N. L. On the Side-Reaction of *N*-Alkylation of Amino-Groups During Hydrogenolytic Deprotection in Alcohol-Containing Solvents. *Int. J. Pept. Protein Res.* **1993**, *41*, 611−611. (c) Mazaleyrat, J. P.; Xie, J.; Wakselman, M. Selective Hydrogenolysis of the Benzyloxycarbonyl Protecting Group of *N*-Epsilon-Lysine in Cyclopeptides Containing a Benzylic Phenyl Ether Function-Evidence for *N*-Epsilon-

Methylated Lysine Side Products. *Tetrahedron Lett.* **1992**, *33*, 4301−4302. (d) Filira, F.; Biondi, L.; Gobbo, M.; Rocchi, R. *N*-Alkylation of Amino Acids During Hydrogenolytic Deprotection. *Tetrahedron Lett.* **1991**, *32*, 7463−7464.

(18) Fredholm, B. B.; Ijzerman, A. P.; Jacobson, K. A.; Klotz, K.-N.; Linden, J. International Union of Pharmacology. XXV. Nomenclature and Classification of Adenosine Receptors. *Pharmacol. Rev.* **2001**, *53*, 527−552.

(19) Buschmann, V.; Weston, K. D.; Sauer, M. Spectroscopic Study and Evaluation of Red-Absorbing Fluorescent Dyes. *Bioconjugate Chem.* **2003**, *14*, 195−204.

(20) Cordeaux, Y.; Briddon, S. J.; Megson, A. E.; McDonnell, J. M.; Dickenson, J. M.; Hill, S. J. Influence of Receptor Number on Functional Responses Elicited by Agonists Acting at the Human Adenosine A(1) Receptor: Evidence for Signaling Pathway-Dependent Changes in Agonist Potency and Relative Intrinsic Activity. *Mol. Pharmacol.* **2000**, *58*, 1075−1084.

(21) For definitions and further details on data analysis, see Pharmacology Methods in the Experimental Section.

(22) Briddon, S. J.; Middleton, R. J.; Yates, A. S.; George, M. W.; Kellam, B.; Hill, S. J. Application of Fluorescence Correlation Spectroscopy to the Measurement of Agonist Binding to a G-Protein Coupled Receptor at the Single Cell Level. *Faraday Discuss.* **2004**, *126*, 197−207.

(23) Rigler, R.; Pramanik, A.; Jonasson, P.; Kratz, G.; Jansson, O. T.; Nygren, P.-Å.; Ståhl, S.; Ekberg, K.; Johansson, B.-L.; Uhlén, S.; Uhlén, M.; Jörnvall, H.; Wahren, J. Specific Binding of Proinsulin C-Peptide to Human Cell Membranes. *Proc. Natl. Acad. Sci. U.S.A.* **1999**, *96*, 13318−13323.

(24) Hampton, A. Nucleotides 2. A New Procedure for Conversion of Ribonucleosides to 2′,3′-*O*-Iisopropylidene Derivatives. *J. Am. Chem. Soc.* **1961**, *83*, 3640−3645.

(25) Baddiley, J. Adenine 5′-Deoxy-5′-methylthiopentoside (Adenine Thiomethyl Pentoside)—A Proof of Structure and Synthesis. *J. Chem. Soc.* **1951**, 1348−1351.

(26) Schmidt, R. R.; Fritz, H.-J. Synthesis and Structure of Inosine-5′-carboxylic Acid and Derivatives. *Chem. Ber.* **1970**, *103*, 1867−1871.

(27) Atwell, G. J.; Denny, W. A. Monoprotection of α,ω-Alkanediamines with the *N*-Benzyloxycarbonyl Group. *Synthesis* **1984**, 1032−1033. For an alternative synthesis, see Pittelkow, M.; Lewinsky, R.; Christensen, J. B. Selective Synthesis of Carbamate Protected Polyamines Using Alkyl Phenyl Carbonates. *Synthesis* **2002**, 2195−2202.

(28) For an alternative synthesis of **5b**, see: (a) Blagborough, I. S.; Moya, E.; Walford, S. P. Practical, Convergent Total Synthesis of Polyamine Amide Spider Toxin NSTX-3. *Tetrahedron Lett.* **1996**, *37*, 551−554. (b) Wälchli-Schaer, E.; Eugster, C. H. Equisetic Alkaloids 17. Synthesis of Threo-*cis*-threo-*trans*-dihydropalustrin and Erythro-*cis*-erythro-*trans*-dihydropalustrin. *Helv. Chim. Acta* **1978**, *61*, 928−935.

(29) Bredereck, H. Über Methylierte Nucleosiden und Purines und Ihre Pharmakologische Wirkungen. I. Methylierung von Nucleosiden durch Diazomethan. *Chem. Ber.* **1947**, *80*, 401−405.

(30) Alexander, S. P.; Cooper, J.; Shine, J.; Hill, S. J. Characterization of the Human Brain Putative A2B Adenosine Receptor Expressed in Chinese Hamster Ovary (CHO, A2B4) cells. *Br. J. Pharmacol.* **1996**, *119*, 1286−1290.

(31) Alvarez, R.; Daniels, D. V. A Single Column Method for the Assay of Adenylate-Cyclase. *Anal. Biochem.* **1990**, *187*, 98−103.

JM061279I